Published in final edited form as:
Macromol Rapid Commun. 2015 February ; 36(3): 332–338. doi:10.1002/marc.201400586.

Chitosan-PEG Hydrogel with Sol–Gel Transition Triggerable by Multiple External Stimuli

Ching Ting Tsao,
Department of Materials Science & Engineering, University of Washington, Seattle, Washington 98195, USA

Meng Hsuan Hsiao,
Department of Materials Science & Engineering, University of Washington, Seattle, Washington 98195, USA

Department of Materials Science and Engineering, National Chiao Tung University, Hsinchu City 300, Taiwan

Mengying Zhang,
Department of Materials Science & Engineering, University of Washington, Seattle, Washington 98195, USA

Sheeny Lan Levengood, and
Department of Materials Science & Engineering, University of Washington, Seattle, Washington 98195, USA

Miqin Zhang
Department of Materials Science & Engineering, University of Washington, Seattle, Washington 98195, USA

Miqin Zhang: mzhang@u.washington.edu

Keywords

hydrogel; chitosan; poly(ethylene glycol); smart gel; biocompatible

Polymers that display a physicochemical response to changes in environmental conditions have been investigated as smart materials.[1] Often a significant change in polymer structure and properties is induced by a small environmental stimulus (*e.g.*, temperature change). This response is generally observed as a change in physicochemical properties such as color, transparency, conductivity, shape (*e.g.*, shape memory), or material state (*e.g.*, sol/gel). One class of these materials, known as environmentally sensitive hydrogels or smart gels, has recently drawn considerable attention. A number of hydrogel systems have been developed that are responsive to physical stimuli such as temperature,[2–4] electric/magnetic fields,[5,6]

Correspondence to: Miqin Zhang, mzhang@u.washington.edu.

Supporting Information
Supporting Information is available from the Wiley Online Library or from the author.

and UV light,[7] or to chemical stimuli such as oxidation/reduction,[8] ionic strength,[9] pH,[10] solvent composition,[11] and exposure to a specific chemical.[12]

A biocompatible hydrogel th at responds to environmental variables in a predictable manner is particularly appealing for biomedical applications.[13] Material responses to changes in temperature, salt concentration, or pH are widely explored because of their relevance to biological systems. For example, sol–gel transition in response to temperature change is useful for injection of a drug-containing hydrogel solution into an irregularly-shaped tissue defect present because of tumor resection. The injected hydrogel solution would respond to the change from room temperature to physiological temperature resulting in formation of a gel that fills the defect. This is useful for regenerative medicine and/or drug delivery applications. This strategy allows for implantation with minimal invasiveness and provides the added benefit of retention in the desired location. A second variable that can affect sol-gel transition properties is salt concentration. Sodium salt is a regulator of blood, body fluids and certain metabolic functions, and an increase in local sodium concentration has been linked to tumor malignancy in human brain[14] and breast tissues.[15] Finally, variation in pH can induce sol-gel transition and in tumor and inflammatory tissues the local environment is more acidic than in normal tissues.[16] Therefore, materials that undergo a physicochemical response to changes in temperature, salt concentration and pH may be of great interest in many biomedical applications. A gradient in temperature between ambient and physiological temperature as well as a gradient in salt concentration or pH between a target pathological tissue and normal tissue can be exploited to trigger hydrogel matrix formation or dissociation (gel-to-sol transition) based on the desired application. Generally, a hydrogel that is responsive to multiple stimuli is a more versatile smart material with broader applications.[17] Thus, it is desirable to develop smart materials with optimal architectures that are responsive to multiple and diverse stimuli in a predictable manner.[18,19] However, due to the challenges associated with the design and synthesis of multi-stimuli-responsive smart materials,[20] most current systems respond only to a single stimulus or are limited to temperature and pH response only. Hydrogels with multi-stimuli responsive ness remain rare[21] and continue to present a challenge.

In this study, we developed a hydrogel (mPEG-g-chitosan) that is responsive to changes in temperature, salt concentration, solute concentration, and pH, all of which are common environmental variables present in biological systems. The primary components of this hydrogel, polyethylene glycol (PEG) and chitosan, are among the most widely used biocompatible polymers.[1, 22] Hydrogels that are both biocompatible and multi-stimuli-responsive are invaluable for biomedical applications. Hydrogels composed of PEG and chitosan possess many advantages compared with those derived from synthetic *N*-Isopropylacrylamide (poly(NiPAAM)) or acidic poly(lactic acid) (PLA).[23] PEG is one of a limited number of synthetic polymers approved by the U.S. Food and Drug Administration (FDA) for incorporation into a variety of foods, cosmetics, personal care products, pharmaceuticals, and biomaterials.[23] Chitosan, a natural, biodegradable polysaccharide derived by the partial deacetylation of chitin, shares structural similarities to the glycosaminoglycans (GAG) present in native extracellular matrix (ECM).[24, 25] Furthermore, the hydrophilicity of chitosan makes it amenable to cell adhesion and

proliferation and its degradation products are non-toxic. In addition, our synthetic approach does not involve an organic solvent. This eliminates possible contamination of mPEG-g-chitosan powder product due to absorption of organic solvent molecules, which is harmful in biological environments.

The detailed preparation and characterization for mPEG-g-chitosan are provided in the Supporting Information. Briefly, mPEG-g-chitosan was synthesized via a two-step reaction: (1) a ring opening reaction of succinic anhydride with mPEG to form mPEG-acid, and (2) amide linkage formation between mPEG-acid and chitosan (Figure 1a-b). The FTIR spectra of mPEG, succinic anhydride and mPEG-acid are shown in Figure 1c. The characteristic adsorption of mPEG at approximately 1150, 2878 and 3500 cm^{-1} indicates ether linkages (–C-O-C–), methylene bridges (–CH_2–), and hydroxyl groups (–OH), respectively.[26] The characteristic adsorption of succinic anhydride at approximately 1820 and 1760 cm^{-1} is associated with the carbonyl group (C=O).[26] The spectrum of the mPEG-g-chitosan featured similar characteristic peaks as those of its parent polymers; compared with that of succinic anhydride, the carbonyl group absorption of mPEG-g-chitosan shifted to 1740 and 1700 cm^{-1}, respectively. The shift of carbonyl absorption also indicates that there was no unreacted succinic anhydride remaining in the mPEG-acid. In Figure 1d, the characteristic adsorption of chitosan around 1050, 1150, 1560, 1655 and 3450 cm^{-1} corresponds to the glycosidic linkage (–C-O-C–) within and between monomers, and to amide II band, amide I band, and to internal hydroxyl group respectively.[27] The spectrum of the mPEG-g-chitosan featured similar characteristic peaks as those of chitosan; the adsorption of carbonyl groups at approximately 1740 cm^{-1} was also observed. Furthermore, the intensity of the amide I and II bands were stronger in mPEG-g-chitosan than in chitosan. The increase in amide I and II bands elucidates the amide linkage formation between chitosan and mPEG-acid, resulting in mPEG-g-chitosan.

The ^{1}H NMR spectrum in Figure S1 confirms the chemical structure of mPEG-acid. The ^{1}H NMR spectrum in Figure 1e-f further confirms that mPEG-acid was incorporated into chitosan as all the peaks unique to mPEG-acid and chitosan are observed. The characteristic assignments of mPEG-g-chitosan are: δ = 4.6–4.7 (H-6), 4.2 (H-4), 3.5–3.7 (H-2, H-3, H-8, H-9, H-10, and H-11), 3.4 (H-1), 3.0–3.2 (H-7), 2.6 (H-5), 2.1 ppm (H-12).[2, 24] The ^{1}H NMR analysis also shows the degree of PEG-grafting (PEGylation) as 18 mol%.

Characterization of the thermoresponsive gelation behavior was carried out using rheological analysis. The sol–gel transition temperature for mPEG-g-chitosan at 1.5 wt% in 1× PBS was determined by the crossover of storage (G') and loss modulus (G") as shown in Figure 2a. As the temperature increased, both G' and G" increased, and the crossover of the two moduli occurred at phase angle (Θ) = 45°. The temperature at which the phase angle and the two moduli cross is defined as the sol–gel transition temperature.[28] Thus, the sol–gel transition temperature for 1.5 wt% mPEG-g-chitosan in 1× PBS, as shown in Figure 2a, is ~28°C. Similarly, to determine their gelation temperatures, the Θ, G' and G" for mPEG-g-chitosan in DI water, 1× PBS, and 10× PBS with different solute concentrations (*i.e.*, mPEG-g-chitosan at 0.5, 1.0, 1.5, 2.0, and 2.5 wt%) were characterized. Figure 2b shows the variation in gelation temperature for mPEG-g-chitosan at different salt and solute concentrations. For all the conditions examined, when heated from 5°C to higher

temperatures, the mPEG-g-chitosan transitioned from a sol (hydrophilic) to gel (hydrophobic) state. The hydrophilicity and hydrophobicity of the hydrogel are governed by hydrogen bonding between mPEG and water molecules and the hydrophobic interaction between chitosan polymer chains, respectively. The intermolecular forces that govern mPEG-g-chitosan behavior are dominated by hydrogen bonding at low temperatures while hydrophobic interactions prevail as the temperature increases.[3]

When higher concentrations of salt were introduced, the sol–gel transition curve shifted to a higher temperature regime. This salt concentration dependence suggests a salt–in (salt–suppressed) behavior, where the salt is not strongly hydrated. Instead, salt replaces some of the water molecules in the hydration shell of the solutes.[29, 30] In other words, the role of the added salt is equivalent to solvent (water). The addition of salt lowers the solute (mPEG-g-chitosan) concentration as the solute becomes more dispersed in the solvent thus reducing the chances of polymer chain interactions.[30] Therefore, it is difficult for mPEG-g-chitosan to form hydrophobic aggregates at the same temperature when heated. To attain gelation, more energy is needed, leading to a higher overall gelation temperature or delayed gelation. This mPEG-g-chitosan system does not exhibit a salt–out (salt–assisted) phenomenon, where salts are strongly hydrated, exhibiting extensive interaction with water.[29] Through the interactions with water, the salts decrease solute solubility, thereby increasing the hydrophobicity of a solute in water. This enhances the gelation process.[30] Furthermore, except in the case of 10× PBS, the increase of the mPEG-g-chitosan concentration from 0.5 to 1.0 wt% elevated the aggregation tendency of mPEG-g-chitosan, resulting in a decrease of the sol–gel transition temperature. That is, the onset of gelation occurred sooner, indicating more efficient packing of mPEG-g-chitosan into stronger networks in ionic solutions. However, a further increase in solute concentration from 1.0 to 2.5 wt% decreased the aggregation tendency and thus the onset of gelation occurred later. This indicates that excessive mPEG-g-chitosan perturbations prevent polymer network formation and subsequent gelation. The inconsistent behavior of the mPEG-g-chitosan in 10× PBS might due to excessive network formation resulting in collapse of the network structure in a highly concentrated salt environment. In summary, the sol–gel transition temperature of mPEG-g-chitosan showed salt and solute concentration dependence.

The sol–gel transition of mPEG-g-chitosan was also dependent on the solution pH. At pH 2.5, 4.0 and 5.5, the storage modulus (G') remained unchanged as the temperature increased (Figure 3a), and the corresponding phase angle did not reach 45° in the tested temperature range (Figure 3b). The sol–gel transition is not observed at pH 2.5, 4.0 and 5.5. On the other hand, at pH 6.5, 7.5 and 8.5, the fact that solutions underwent a sol–gel transition was verified by an increase in storage modulus and decrease in phase angle with temperature elevation. The storage modulus, also known as elastic modulus, is important for characterizing the mechanical properties of viscoeastic materials.[31] The sol–gel transition of pH 8.5 hydrogel occurred at 35°C and the corresponding storage modulus was 80 times higher than that of pH 2.5 hydrogel, suggesting that the pH 8.5 hydrogel is firmer and easier to handle compared with its counterpart post-gelation. Figure 3c shows the 1.5 wt% mPEG-g-chitosan at 37°C with pH values of 4.0, 7.5 and 8.5, respectively. At pH 4.0, the solution exists in a transparent sol state. As pH increased to 7.5 and 8.5, the solution underwent a sol– gel transition, and became a stationary, non-flowing gel. Furthermore, the charge state

of the polymer was evaluated with zeta potential measurements. Figure 3e shows the zeta potential of 1.5 wt% mPEG-g-chitosan with different pH values. mPEG-g-chitosan exhibited cationic potential at pH of 2.5, 4.0, and 5.5, and near neutral potential at pH 6.5, 7.5 and 8.5. The presence of ionic components within chitosan is believed to impart pH-sensitivity to the hydrogels.[32] Protonation or deprotonation of chitosan amines in association with pH changes above or below the amine's pK_a value (6.5)[33] produced a small variation in the balance between hydrophilicity and hydrophobicity resulting in a substantial change for the phase transition temperature.[34] At pHs below the pK_a value, chitosan amines were protonated and likely interacted strongly with water thus preventing the mPEG-g-chitosan chains from undergoing packing and subsequent gelation. At pHs higher than the pK_a value, chitosan amines were deprotonated and unionized, stimulating chitosan dehydration and resulting in the formation of a hydrophobic network and the eventually formation of the gel phase. Figure 3d shows the injectability of 1.5 wt% mPEG-g-chitosan at pH 7.5. At 4°C, the solution flows easily and can be injected without bubble formation (inset, left). At 37°C, 1.5 wt% mPEG-g-chitosan in the gel state is not easily drawn up with a syringe and when injected, air bubble formation is significant (inset, right).

The effect of various stimuli evaluated herein on mPEG-g-chitosan sol–gel transition is schematically elucidated in Figure S2. mPEG-g-chitosan chains are randomly distributed at lower temperatures (4°C) and dominated by hydrophilic interactions. As temperature increases (37°C), the added thermal energy promotes polymer chain rearrangement allowing a transition into dominance of hydrophobic interactions. Driven by hydrophobic interactions, the mPEG-g-chitosan chains form aggregates, resulting in the formation of a gel network (Figure S2a). When salt is introduced, fewer hydrophobic interactions are observed since the salts play a similar role as the solvent (water) (Figure S2b). When salts are present, polymer chain aggregation due to hydrophobic interactions does not occur as easily as the no-salt system at a given temperature. Thus more energy is required for gelation with the introduction of salts resulting in gelation at higher temperature (>37°C). With an increase in mPEG-g-chitosan concentration, a gel network forms more easily due to an increased probability of polymer-polymer interactions and gelation occurs at lower temperature (<37°C) (Figure S2c). However, further increases in mPEG-g-chitosan concentration disrupts network formation (Figure S2d). High concentrations of mPEG-g-chitosan interrupt optimal polymer packing thereby preventing gel formation. The amine on mPEG-g-chitosan becomes protonated when the pH of the system falls below the pK_a of chitosan (Figure S2e). Thus the hydrophobic interactions among polymer chains required for packing and gel network formation are diminished due to repulsive electrostatic forces among protonated chitosan amines. Gel formation is more difficult owing to decreased polymer chain interactions.

The release profile for a model protein incorporated in the gel and the biocompatibility of mPEG-g-chitosan are presented in Figure S3a and b, **respectively**. The porous microstructure of mPEG-g-chitosan is presented in Figure S3c. These preliminary results demonstrate the potential of mPEG-g-chitosan for tissue engineering and drug delivery applications.

In summary, we demonstrated the successful synthesis of a mPEG-g-chitosan gel, which exhibits rheological properties consistent with multi-stimuli sensitivity. The sol–gel transition of mPEG-g-chitosan is attributable to the delicate changes in the balance between hydrophilicity and hydrophobicity. The sol–gel transition of mPEG-g-chitosan is salt concentration, solute concentration, temperature, and pH dependent. As such, the sol–gel transition temperature can be easily regulated by controlling these three variables to meet the requirements of target applications. The sol–gel transition mechanisms illustrated in this study may be helpful for design of other smart gels.

Supplementary Material

Refer to Web version on PubMed Central for supplementary material.

Acknowledgements

This work is supported in part by NIH grant NIH/NCI R01CA172455 and Kyocera Professor Endowment to M.Z. M.H. acknowledges support by the National Science Council, Taiwan. S.L.L. acknowledges support from the Ruth L. Kirschstein NIH Training grant T32CA138312. We acknowledge the use of resources at the Center for Nanotechnology and Department of Immunology at the University of Washington.

References

1. Bhattarai N, Gunn J, Zhang M. Adv. Drug Deliv. Rev. 2010; 62:83. [PubMed: 19799949]
2. Bhattarai N, Matsen FA, Zhang M. Macromol. Biosci. 2005; 5:107. [PubMed: 15719428]
3. Bhattarai N, Ramaya HR, Gunna J, Matsen FA, Zhang M. J. Control. Release. 2005; 103:609. [PubMed: 15820408]
4. Chen SH, Tsao CT, Chang CH, Wu YM, Liu ZW, Lin CP, Wang CK, Hsieh KH. Carbohydr. Polym. 2012; 88:1483.
5. Brazel CS. Pharm. Res. 2009; 26:644. [PubMed: 19005741]
6. Zhang Y, Yang B, Zhang X, Xu L, Tao L, Lia S, Wei Y. Chem. Commun. 2012; 48:9305.
7. Peng K, Tomatsu I, v.d. Broek B, Cui C, Korobko AV, v. Noort J, Meijer AH, Spaink HP, Kros A. Soft Matter. 2011; 7:4881.
8. Jin L, Zhao YJ, Liu X, Wang YL, Ye BF, Xie ZY, Gu ZZ. Soft Matter. 2012; 8:4911.
9. Zhang R, Tang M, Bowyer A, Eisenthal R, Hubble J. Biomaterials. 2005; 26:4677. [PubMed: 15722138]
10. Betz M, Hormansperger J, Fuchs T, Kulozik U. Soft Matter. 2012; 8:2477.
11. Ozturk V, Okay O. Polymer. 2002; 43:5017.
12. Miyata T, Asami N, Uragami T. Nature. 1999; 399:766. [PubMed: 10391240]
13. Guan Y, Zhao H, Yu L, Chen S, Wang Y. RSC Adv. 2014; 4:4955.
14. Ouwerkerk R, Bleich KB, Gillen JS, Pomper MG, Bottomley PA. Radiology. 2003; 227:529. [PubMed: 12663825]
15. Ouwerkerk R, Jacobs MA, Macura KJ, Wolff AC, Stearns V, Mezban SD, Khouri NF, Bluemke DA, Bottomley PA. Breast Cancer Res. Treat. 2007; 106:151. [PubMed: 17260093]
16. Kohman RE, Cha CY, Zimmerman SC, Kong HJ. Soft Matter. 2010; 6:2150. [PubMed: 20694176]
17. Hu JM, Liu SY. Macromolecules. 2010; 43:8315.
18. Zhang Y, Tao L, Li S, Wei Y. Biomacromolecules. 2011; 12:2894. [PubMed: 21699141]
19. Yan X, Xu D, Chi X, Chen J, Dong S, Ding X, Yu Y, Huang F. Adv. Mater. 2012; 24:362. [PubMed: 22161963]
20. Schattling P, Jochum FD, Theato P. Chem. Commun. 2011; 47:8859.
21. Tan L, Liu Y, Ha W, Ding LS, Peng SL, Zhang S, Li BJ. Soft Matter. 2012; 8:5746.
22. Jeong B, Bae YH, Lee DS, Kim SW. Nature. 1997; 388:860. [PubMed: 9278046]

23. Jeong B, Kim SW, Bae YH. Adv. Drug Deliv. Rev. 2002; 54:37. [PubMed: 11755705]
24. Tsao CT, Kievit FM, Ravanpay A, Erickson AE, Jensen MC, Ellenbogen RG, Zhang M. Biomacromolecules. 2014; 15:2656. [PubMed: 24890220]
25. Tsao CT, Kievit FM, Wang K, Erickson AE, Ellenbogen RG, Zhang M. Mol. Pharm. 2014; 11:2134. [PubMed: 24779767]
26. Chen SH, Tsao CT, Chang CH, Lai YT, Wu MF, Liu ZW, Chuang CN, Chou HC, Wang CK, Hsieh KH. Macromol. Mater. Eng. 2013; 298:429.
27. Muyonga JH, Cole CGB, Duodu KG. Food Chem. 2004; 86:353.
28. Bulcke AIVD, Bogdanov B, Rooze ND, Schacht EH, Cornelissen M, Berghmans H. Biomacromolecules. 2000; 1:31. [PubMed: 11709840]
29. Xu Y, Wang C, Tam KC, Li L. Langmuir. 2004; 20:646. [PubMed: 15773087]
30. Kundu SK, Yoshida M, Shibayama M. J. Phys. Chem. B. 2010; 114:1541. [PubMed: 20055469]
31. Chiu YL, Chen SC, Su CJ, Hsiao CW, Chen YM, Chen HL, Sung HW. Biomaterials. 2009; 30:4877. [PubMed: 19527916]
32. Fu C, Wang S, Feng L, Liu X, Ji Y, Tao L, Li S, Wei Y. Adv. Healthc. Mater. 2013; 2:302. [PubMed: 23184363]
33. Hsu LW, Lee PL, Chen CT, Mi FL, Juang JH, Hwang SM, Ho YC, Sung HW. Biomaterials. 2012; 33:6254. [PubMed: 22681978]
34. Lee SY, Lee Y, Kim JE, Park TG, Ahn CH. J. Mater. Chem. 2009; 19:8198.

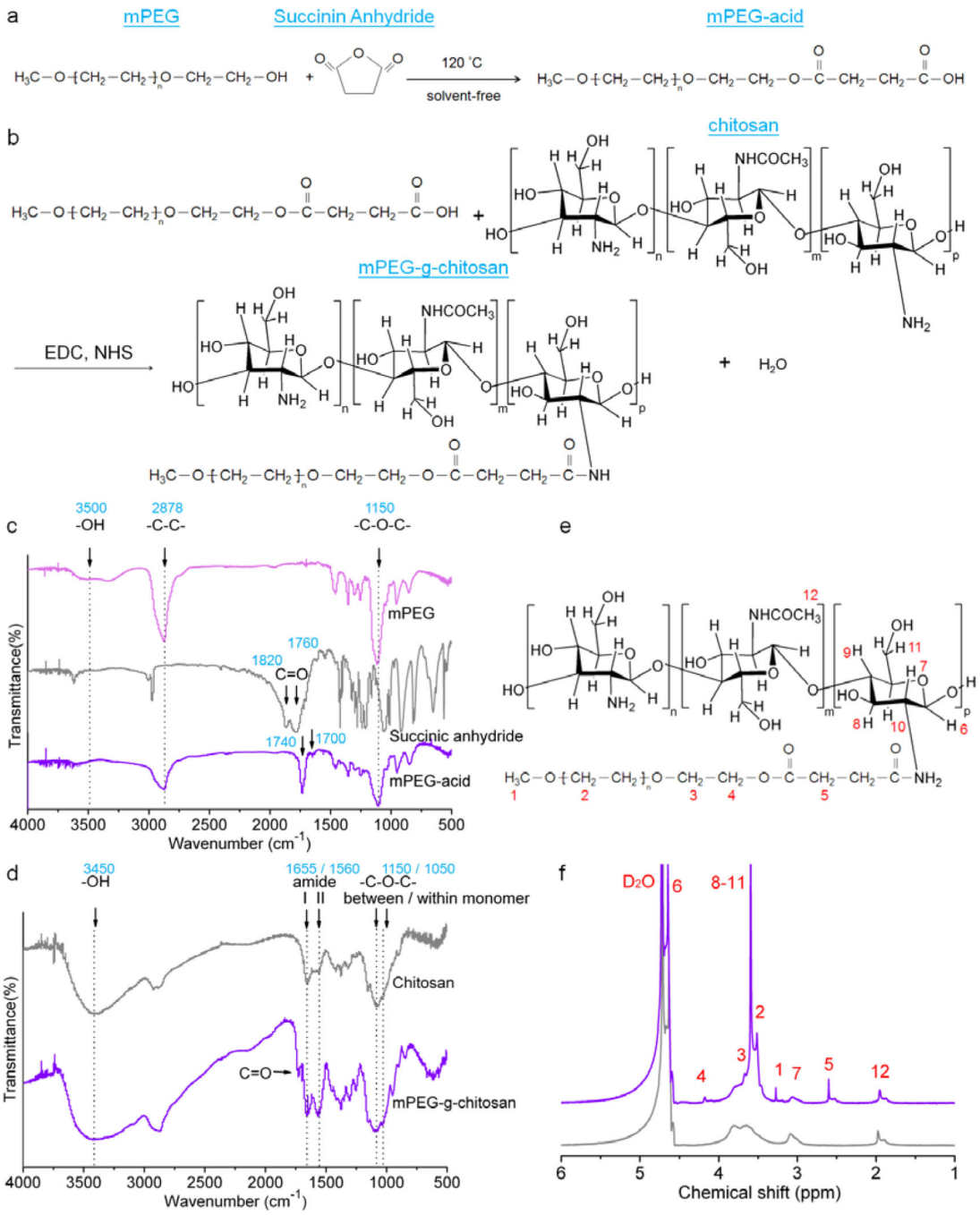

Figure 1.

Synthetic route and chemical structures of mPEG-acid and mPEG-g-chitosan. Schematic representation of chemical reactions producing (**a**) mPEG-acid and (**b**) mPEG-g-chitosan; FTIR spectra of (**c**) mPEG, succinic anhydride and mPEG-acid, and (**d**) chitosan and mPEG-g-chitosan; (**e**) Chemical structure of mPEG-g-chitosan, and (**f**) ^{1}H NMR spectra of mPEG-g-chitosan (purple) and pure chitosan (gray).

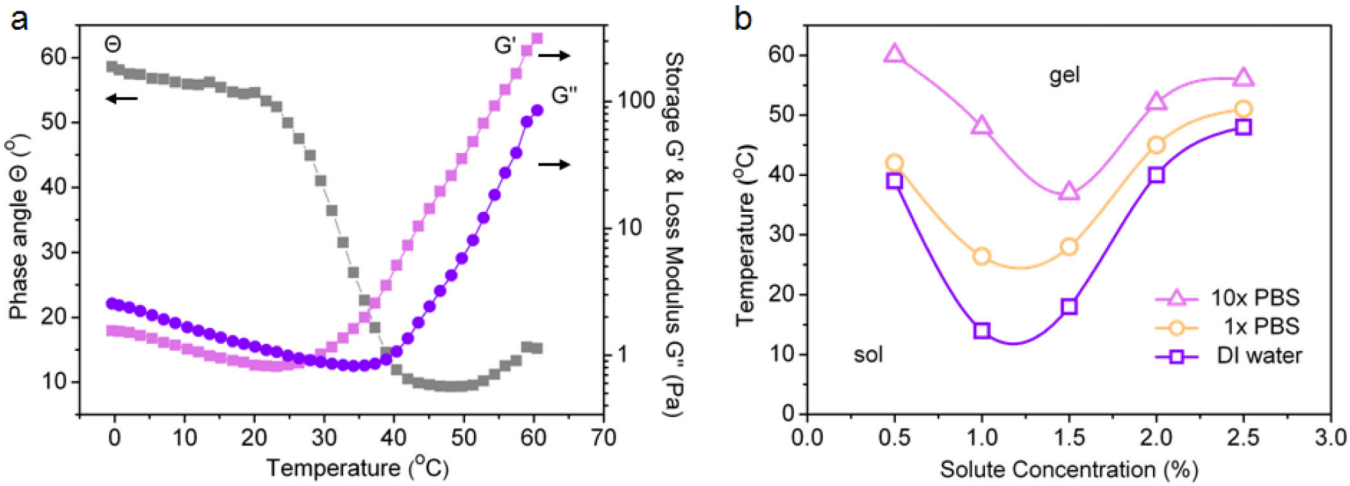

Figure 2.

Rheological properties of mPEG-g-chitosan: (a) Phase angle, storage and loss moduli as a function of temperature for 1.5 wt% mPEG-g-chitosan in 1× PBS; (b) Phase transition diagrams of mPEG-g-chitosan in the presence of different salt concentrations (DI water, 1× PBS, 10× PBS) with different solute concentrations (mPEG-g-chitosan at 0.5, 1.0, 1.5, 2.0, and 2.5 wt%). For 2a, frequency: 1Hz; strain: 10%; temperature ramping: 1°C/min.

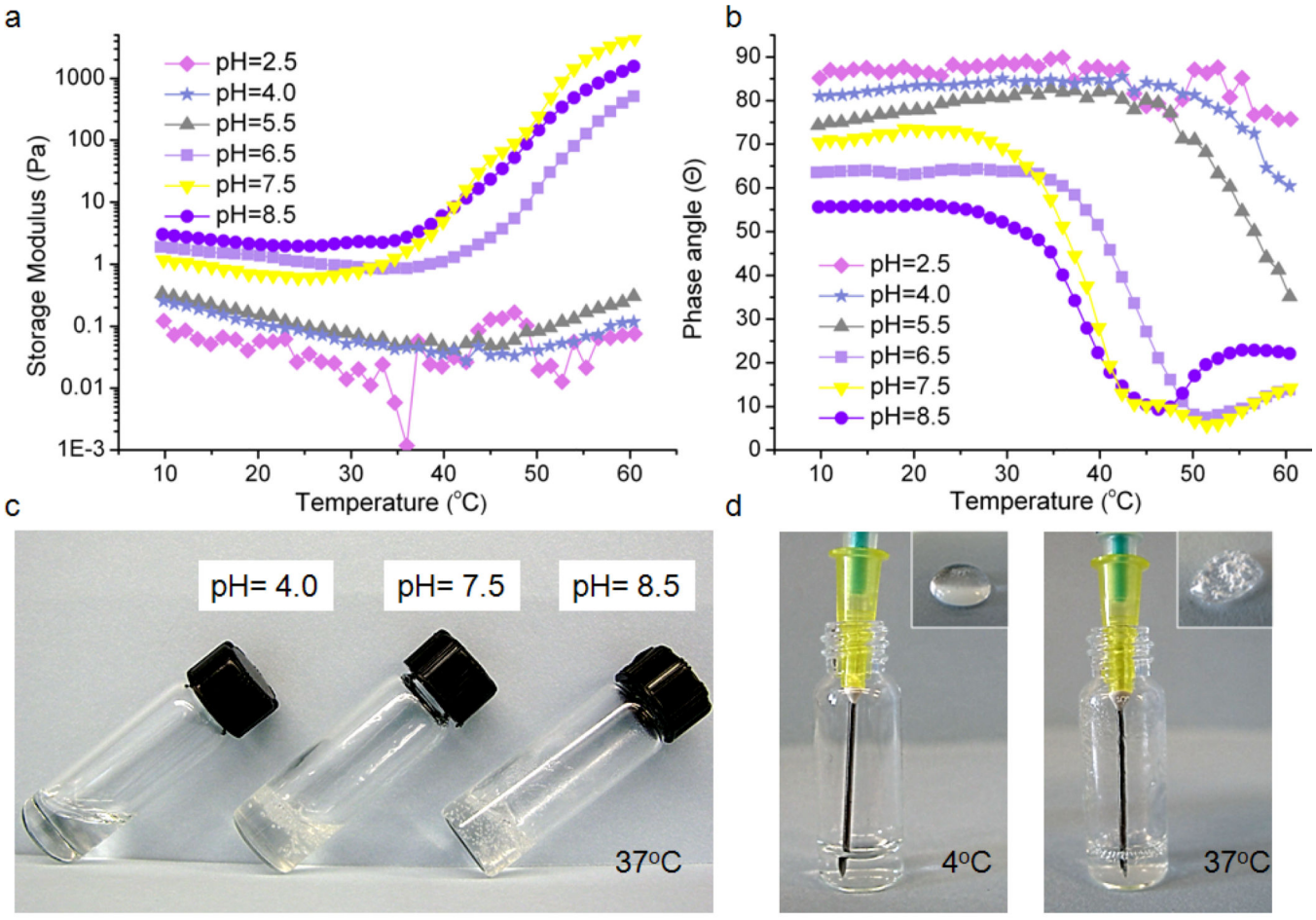

e

	pH value					
	2.5	4.0	5.5	6.5	7.5	8.5
Zeta Potential (mV)	17.83 ± 1.71	6.62 ± 0.88	6.69 ± 0.59	3.84 ± 0.54	-1.39 ± 0.53	-3.82 ± 0.79

Figure 3.

The effect of pH on physical properties of mPEG-g-chitosan (1.5 wt%): (a) storage modulus, and (b) phase angle as a function of temperature; (c) appearance of gels of different pHs at 37°C, (d) gel injectability via syringe at 4°C and 37°C (1.5 wt%, pH 7.5), (e) zeta potential as a function of pH value. For 3a and 3b, frequency: 1Hz; strain: 10%; temperature ramping: 1°C/min.